MRGF: A robust SLAM Framework based on Millimeter wave Radar and GNSS Fusion in Harsh Environments

Fangcheng Qu[1], Yuheng Zhang [3], Xianlang Wei[4], Youchen Tang[5], Jian Zhou[2,5,*]

[1] Wuhan University, School of Geodesy and Geomatics, 430074 Wuhan, China - fang_cheng@whu.edu.cn
[2] Hubei Luojia laboratory, 430074 Wuhan
[3] Wuhan University, College of Earth and Space Sciences, 430074 Wuhan, China - zyh2024@whu.edu.cn
[4] Wuhan University, School of Electronic Information, 430074 Wuhan, China - 2024302121152@whu.edu.cn
[5] Wuhan University, State Key Laboratory of Information Engineering in Surveying, Mapping and Remote Sensing, 430074 Wuhan, China - (youchentang, jianzhou)@whu.edu.cn

Keywords: Multi-band radar, Complementary Sensor fusion, Pose graph optimization

ABSTRACT

Maritime vehicles face significant positioning challenges under adverse weather conditions where visual and laser SLAM systems suffer from severe degradation. Millimeter-wave radar offers inherent robustness to weather interference, yet single-band radar cannot simultaneously achieve accurate translation and robust attitude estimation.This paper proposes a complementary fusion framework for multi-band radar odometry.This system leverages W-band radar (CFEAR) for reliable translation estimation and combines it with X-band radar (LodeStar) to improve rotational estimation robustness. The main innovations are as follows:(1) A complementary fusion framework exploiting the complementary characteristics of W-band and X-band radar; (2) A quality-aware adaptive weighting mechanism dynamically computing fusion weights based on sensor data quality assessment; (3) A consistency gating mechanism monitoring inter-sensor agreement and activating protective measures during sensor degradation.Experiments on the MOANA maritime dataset demonstrate that the proposed method achieves stable and reliable local motion estimation, reaching an RTE RMSE of 1.67 m on the Near-Port sequence.

1 Introduction

Robust localization and mapping in maritime environments remains a critical challenge for autonomous navigation systems. Under adverse conditions such as heavy rain, fog, sea clutter, and dynamic platform motion, reliable ego-localization is essential for navigation safety and mission reliability [1]. However, conventional perception systems degrade significantly in such scenarios. Visual SLAM methods are sensitive to illumination changes and texture scarcity, leading to unstable feature tracking and drift [2, 3], while LiDAR-based approaches are affected by scattering, attenuation, and water surface reflections, resulting in reduced measurement reliability [4].

Radar-based SLAM has recently emerged as a promising solution due to its robustness to adverse weather and long-range sensing capability. Methods such as CFEAR achieve LiDAR-level odometry accuracy through conservative filtering and geometric registration [5, 6], while LodeStar improves rotational estimation in maritime radar imagery via radial descriptors [7]. Furthermore, multi-sensor fusion approaches (e.g., radar-inertial and radar-vision SLAM) demonstrate that complementary sensing can enhance robustness [8, 9].

Despite these advances, three key limitations remain. First, single-band radar suffers from an inherent trade-off between resolution and range: high-frequency radars provide accurate short-range estimation but degrade at long distances, whereas low-frequency radars offer extended range but limited spatial precision [10]. Second, existing methods often rely on single-modality or loosely coupled fusion, underutilizing cross-band complementarity. Third, fixed or heuristic fusion strategies lack adaptability to dynamic environmental changes and sensor degradation.

To address these issues, we propose a complementary multi-band radar SLAM framework that tightly integrates W-band and X-band radar. W-band radar is used for accurate translation estimation via CFEAR, while X-band radar provides robust attitude estimation through LodeStar. A quality-aware adaptive weighting mechanism dynamically adjusts sensor contributions, and a consistency gating strategy ensures robustness under sensor degradation.

The main contributions are summarized as follows:

- We propose a complementary multi-band radar fusion framework that tightly integrates W-band and X-band radar, explicitly leveraging their distinct sensing characteristics to overcome the inherent resolution–range trade-off in single-band radar SLAM.
- We develop a quality-aware adaptive weighting strategy that dynamically adjusts the contribution of each radar modality based on real-time estimation confidence, enabling robust and flexible fusion under varying environmental conditions.

- We introduce a consistency gating mechanism that monitors inter-sensor agreement and detects potential degradation, effectively suppressing unreliable measurements and improving overall system stability and long-term localization accuracy.

2 Related Work

2.1 Radar-based SLAM

Radar-based SLAM has emerged as a promising solution for robust localization in adverse environments due to its resilience to weather and long-range sensing capability. Early works focused on adapting classical geometric registration techniques to radar data. For instance, Cen and Newman proposed scan matching methods tailored for FMCW radar, demonstrating the feasibility of radar odometry in large-scale outdoor environments [11]. Building on this, Barnes *et al.* introduced RadarSLAM, which leverages probabilistic scan matching and loop closure to achieve globally consistent mapping using automotive radar [12].

More recent approaches aim to improve robustness and accuracy under noisy and sparse radar measurements. The CFEAR framework introduces conservative filtering and point-to-line registration to suppress spurious radar returns, achieving LiDAR-level localization accuracy across diverse environments [5,6]. In parallel, learning-based and descriptor-based methods have been explored to address the lack of discriminative features in radar data. For example, Scan Context has been adapted to radar for loop detection, enabling efficient place recognition in large-scale scenarios [13]. More recently, LodeStar proposes a radial descriptor tailored for maritime radar imagery, improving rotational estimation stability in low-texture and near-binary radar observations [7].

These methods demonstrate that radar can achieve competitive performance compared to LiDAR and vision in challenging environments. However, most existing radar SLAM systems rely on a single radar modality, limiting their ability to balance resolution, range, and robustness across diverse operational conditions.

2.2 Multi-Sensor Fusion for SLAM

To overcome the limitations of individual sensors, multi-sensor fusion has become a dominant trend in SLAM research. Visual-inertial SLAM systems, such as VINS-Mono, tightly couple camera and IMU measurements to achieve accurate and drift-reduced state estimation [14]. Similarly, LiDAR-inertial systems such as LIO-SAM integrate LiDAR odometry with IMU pre-integration and factor graph optimization, significantly improving robustness in dynamic and large-scale environments [15].

In the radar domain, fusion approaches have also been explored to enhance localization performance. Radar-inertial SLAM methods integrate radar measurements with IMU to compensate for motion distortion and improve short-term state estimation [12]. Radar-vision fusion approaches further exploit complementary sensing characteristics, where vision provides rich texture information while radar ensures robustness under adverse weather conditions [9]. These methods demonstrate that complementary sensing can significantly improve system performance compared to single-modality approaches.

Nevertheless, existing fusion strategies are primarily designed for heterogeneous sensors (e.g., vision–IMU, LiDAR–IMU), while fusion within the radar domain remains underexplored. In particular, the complementary characteristics across different radar frequency bands have not been fully exploited.

2.3 Multi-Band Radar and Maritime SLAM Challenges

Recent advances in radar hardware have enabled the deployment of multi-band radar systems, providing new opportunities for robust perception. High-frequency radars (e.g., W-band) offer high spatial resolution and accurate short-range measurements, whereas low-frequency radars (e.g., X-band) provide long-range sensing and strong penetration capability in adverse weather conditions [10]. This complementary property suggests that multi-band radar fusion has the potential to overcome the inherent limitations of single-band systems.

At the same time, maritime environments introduce additional challenges, including dynamic wave motion, sparse structural features, strong reflections from water surfaces, and rapidly changing environmental conditions. Recent datasets such as MOANA highlight these challenges and demonstrate that existing radar SLAM methods still suffer from degraded performance in long-range and low-feature scenarios [10].

Despite the potential advantages of multi-band radar, existing approaches either rely on single-band sensing or adopt loosely coupled fusion strategies, which fail to fully exploit cross-band complementarity. Moreover, current fusion methods typically employ fixed weighting or heuristic switching, lacking the ability to adapt to dynamically varying sensor quality and environmental conditions.

In summary, prior work has demonstrated strong progress in radar SLAM and multi-sensor fusion. However, three key limitations remain: (1) single-band radar systems cannot simultaneously achieve high-resolution and long-range robustness; (2) cross-band radar fusion is insufficiently explored; and (3) existing fusion strategies lack adaptability and robustness under sensor degradation. These limitations motivate the proposed complementary multi-band radar fusion framework, which explicitly exploits cross-band characteristics through adaptive weighting and consistency-aware gating mechanisms.

https://doi.org/10.5194/isprs-archives-XLIX-B1-2026-647-2026 | © Author(s) 2026. CC BY 4.0 License.

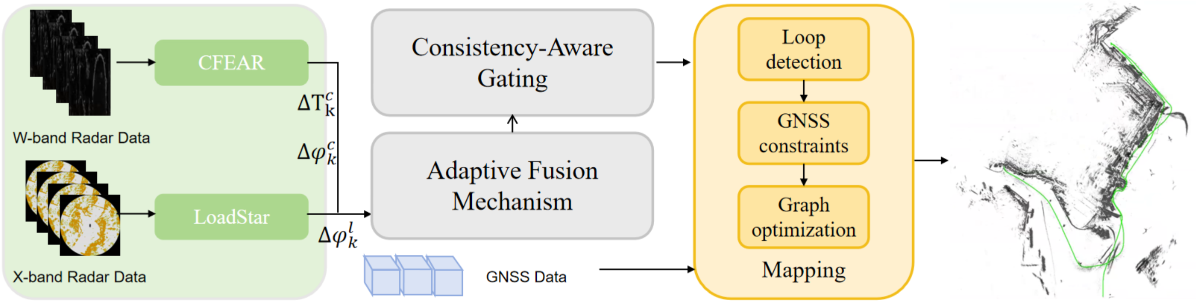

Figure 1 The proposed Multi-Band Radar SLAM framework comprises three tightly coupled stages. (1) **Front-end Processing** (green): W-band radar data is processed by CFEAR to produce relative pose changes (ΔT_k^c) and heading changes ($\Delta\phi_k^c$), while X-band radar data is processed by LodeStar to generate independent heading estimates ($\Delta\phi_k^l$). (2) **Adaptive Fusion and Consistency Gating** (gray): The adaptive fusion mechanism dynamically weights the contributions from both radar modalities based on real-time quality assessment, while the consistency-aware gating module filters out physically inconsistent measurements to prevent error propagation. (3) **Mapping and Back-end Optimization** (yellow): A factor graph optimizer integrates the gated radar odometry with GNSS constraints and loop closure detections to produce globally consistent trajectory and map estimation.

3 Methodology

3.1 Overview for Multi-Band Radar Fusion

To address the degradation of single-modality radar odometry in maritime environments, we design a complementary multi-band radar SLAM framework that explicitly exploits the heterogeneous characteristics of W-band and X-band radar.

The system consists of three tightly coupled components: (1) a dual-band radar frontend that produces complementary motion estimates; (2) a quality-aware fusion module that adaptively combines these estimates; (3) a factor-graph backend integrating radar, GNSS, and optional map constraints.

Given two radar odometry outputs at time k:

$$\Delta T_k^c = (\Delta \mathbf{R}_k^c, \Delta \mathbf{t}_k^c), \quad \Delta\psi_k^l$$

where: ΔT_k^c is the motion estimated by W-band radar (CFEAR), $\Delta\psi_k^l$ is the yaw increment from X-band radar (LodeStar),

the goal is to estimate a robust fused motion:

$$\Delta T_k^f = (\Delta\psi_k^f, \Delta \mathbf{t}_k)$$

that remains stable under noise, sparsity, and sensor degradation.

3.2 Complementarity-Aware Translation and Attitude Decoupling

Due to the intrinsic frequency-dependent sensing characteristics, W-band radar provides high-resolution short-range measurements, while X-band radar offers stable long-range structural cues. Instead of treating both sensors symmetrically, we explicitly decouple translation and rotation estimation.

Translation Estimation. Translation is directly taken from W-band radar:

$$\Delta \mathbf{t}_k = \Delta \mathbf{t}_k^c \tag{1}$$

This choice avoids introducing large-scale drift from X-band radar, whose coarse resolution leads to unreliable displacement estimation.

Attitude Estimation. For rotation, we combine both sources:

$$\Delta\psi_k^f = (1-\alpha_k)\Delta\psi_k^c + \alpha_k \Delta\psi_k^l \tag{2}$$

where: $\Delta\psi_k^c$ is the yaw increment derived from $\Delta \mathbf{R}_k^c$, $\Delta\psi_k^l$ is the LodeStar rotation, $\alpha_k \in [0,1]$ is the fusion weight.

This formulation can be interpreted as a convex combination that biases toward the more reliable sensor at each time step.

The global yaw is then recursively integrated:

$$\psi_k = \psi_{k-1} + \Delta\psi_k^f \tag{3}$$

ensuring temporal consistency.

3.3 Quality-Aware Adaptive Fusion Mechanism

A key challenge is that radar performance varies significantly with environment (e.g., sea clutter, sparsity). Fixed fusion weights fail to adapt to such dynamics. Therefore, we introduce a quality-driven weighting scheme.

Each sensor produces a confidence score:

$$q_k^c \in [0,1], \quad q_k^l \in [0,1]$$

where: q_k^c reflects registration residual consistency in CFEAR, q_k^l measures peak sharpness in LodeStar correlation.

To balance the two sources, we define:

$$\alpha_k = \text{clip}\left(\frac{q_k^l}{q_k^l + \lambda q_k^c}, \alpha_{\min}, \alpha_{\max}\right) \tag{4}$$

where: λ balances the relative scale between two quality metrics, $\alpha_{\min}, \alpha_{\max}$ prevent extreme dominance.

This formulation follows a normalized confidence ratio: when X-band quality q_k^l increases, α_k grows, giving more weight to $\Delta\psi_k^l$. Conversely, when W-band is more reliable, α_k decreases.

The clipping operation ensures numerical stability and prevents abrupt switching.

3.4 Consistency-Aware Gating for Degeneration Suppression

Even with adaptive weighting, severe sensor failures may still introduce outliers. To mitigate this, we introduce an inter-sensor consistency constraint.

We define the rotational discrepancy:

$$\delta_k = |\Delta\psi_k^l - \Delta\psi_k^c| \tag{5}$$

If δ_k exceeds a threshold τ_ψ, the two sensors are considered inconsistent. In such cases, blindly trusting the adaptive weight may amplify errors.

Therefore, we enforce:

$$\alpha_k \to \alpha_{\min}$$

when: $\delta_k > \tau_\psi$, and q_k^l is low.

Additionally: if CFEAR degenerates (low inlier ratio), we relax the upper bound $\alpha_{\max}$, if LodeStar correlation is ambiguous, we cap α_k.

This mechanism effectively introduces a soft decision boundary that suppresses unreliable measurements without hard switching, preserving continuity.

3.5 Factor Graph Optimization with GNSS and Map Constraints

To ensure global consistency, the fused odometry is integrated into a factor graph framework.

We estimate the trajectory:

$$\mathbf{x} = \{x_0, x_1, \ldots, x_n\}$$

by minimizing:

$$\begin{aligned} x^* = \arg\min_{\mathbf{x}} \sum_j \|e_{\text{odom}}(x_j, x_{j+1})\|^2_{\Omega_o} \\ + \sum_k \|e_{\text{GNSS}}(x_k)\|^2_{\Omega_g} \\ + \sum_m \rho\left(\|e_{\text{loop}}(x_m, x_n)\|^2_{\Omega_l}\right) \\ + \sum_s \rho\left(\|e_{\text{map}}(x_s)\|^2_{\Omega_m}\right) \end{aligned} \tag{6}$$

where:

$e_{\text{odom}}(x_j, x_{j+1})$ encodes the fused radar motion ΔT_k^f, $e_{\text{GNSS}}(x_k)$ constrains absolute position from GNSS (mandatory), e_{loop} enforces loop closure consistency, e_{map} aligns poses to a prior map (optional), Ω_* are information matrices representing confidence, $\rho(\cdot)$ is a robust kernel (e.g., Huber) to suppress outliers.

GNSS Factor. The GNSS residual is defined as:

$$e_{\text{GNSS}}(x_k) = \mathbf{p}_k - \mathbf{p}_k^{\text{GNSS}} \tag{7}$$

where $\mathbf{p}_k$ is the estimated position and $\mathbf{p}_k^{\text{GNSS}}$ is the measurement.

This provides global drift correction, which is critical in long-range maritime scenarios.

Map Matching Factor (Optional). When a prior map is available, we define:

$$e_{\text{map}}(x_s) = \mathbf{p}_s - \mathbf{p}_s^{\text{map}} \tag{8}$$

which anchors the trajectory to known structures, improving long-term consistency.

Overall, the backend integrates local radar accuracy with global absolute constraints, forming a robust optimization framework.

Beyond the formulation above, it is worth noting that the proposed framework is designed to explicitly exploit the complementary sensing characteristics across different radar frequency bands. Rather than treating multiple sensors in a symmetric manner, the system assigns distinct roles to each modality, allowing translation and rotation to be estimated through the most reliable source. This design not only improves robustness under adverse maritime conditions, but also provides a flexible foundation for extending the framework to additional sensing modalities such as IMU or prior maps.

4 Experiments and Analysis

4.1 Experimental Datasets

Experiments are conducted on the MOANA (Multi-Radar Dataset for Maritime Odometry and Autonomous Navigation Application) dataset. The MOANA dataset encompasses Port Sequences (Near Port, Outer Port) and Island Sequences (Single Island, Twins Island, Complex Island, Island Expedition, Seaside). In this work, experiments are conducted on the $1_Near_Portsequenceforvalidation.$

Sensor configuration includes W-band radar (Navtech RAS6, 76–77 GHz, 0.175 m resolution, 600 m range, 4 Hz), X-band radar (SIMRAD HALO4, 9.4–9.5 GHz, 2.44–3.25 m/px resolution, 2498–3328 m range, 1 Hz), and GNSS receiver (Hemisphere V500) for ground truth.

4.2 Evaluation Metrics

To quantitatively evaluate the localization performance, we adopt standard trajectory-based metrics widely used in SLAM, including Absolute Trajectory Error (ATE) and Relative Translational Error (RTE). These metrics respectively capture global consistency and local motion accuracy, which are both critical in large-scale maritime environments.

https://doi.org/10.5194/isprs-archives-XLIX-B1-2026-647-2026 | © Author(s) 2026. CC BY 4.0 License.

Before evaluation, the estimated trajectory is temporally synchronized and aligned to the reference trajectory through a rigid transformation. Let $\mathbf{P}_i \in SE(2)$ denote the ground-truth pose at time i, and $\hat{\mathbf{P}}_i \in SE(2)$ the corresponding estimated pose. The operator $\mathrm{trans}(\cdot)$ extracts the translational component of a pose, and N denotes the total number of poses.

Absolute Trajectory Error (ATE).

ATE evaluates the global consistency of the estimated trajectory with respect to the ground truth, and is particularly sensitive to long-term drift. For each time step i, the translational error is defined as

$$e_i^{\mathrm{ATE}} = \left\| \mathrm{trans}\left(\mathbf{P}_i^{-1} \hat{\mathbf{P}}_i \right) \right\|_2 , \tag{9}$$

which measures the deviation between the estimated pose and the reference after alignment.

The overall ATE is computed as the root mean square error (RMSE):

$$\mathrm{ATE}_{\mathrm{RMSE}} = \sqrt{\frac{1}{N} \sum_{i=1}^{N} \left(e_i^{\mathrm{ATE}} \right)^2 }. \tag{10}$$

A lower ATE indicates better global consistency of the trajectory.

Relative Translational Error (RTE).

While ATE reflects accumulated drift, it does not fully capture local motion accuracy. To address this, we additionally evaluate the Relative Translational Error (RTE), which measures short-term consistency over a fixed interval Δ.

The relative pose error between two time steps i and $i + \Delta$ is defined as

$$\mathbf{E}_i = \left(\mathbf{P}_i^{-1} \mathbf{P}_{i+\Delta} \right)^{-1} \left(\hat{\mathbf{P}}_i^{-1} \hat{\mathbf{P}}_{i+\Delta} \right). \tag{11}$$

The translational component of this error is then given by

$$e_i^{\mathrm{RTE}} = \left\| \mathrm{trans}(\mathbf{E}_i) \right\|_2 , \tag{12}$$

which reflects the discrepancy between the estimated and ground-truth motion over the interval.

The RMSE over all valid pairs ($M = N - \Delta$) is computed as

$$\mathrm{RTE}_{\mathrm{RMSE}} = \sqrt{\frac{1}{M} \sum_{i=1}^{M} \left(e_i^{\mathrm{RTE}} \right)^2 }. \tag{13}$$

Compared to ATE, RTE is less sensitive to global alignment and better reflects short-term drift behavior.

RMSE (General Form).

For completeness, given a sequence of errors $\{e_i\}$, the root mean square error is defined as

$$\mathrm{RMSE} = \sqrt{\frac{1}{K} \sum_{i=1}^{K} e_i^2 }. \tag{14}$$

This metric provides a unified way to summarize the magnitude of estimation errors.

4.3 Main Results

Figure 2 Trajectory comparison on the Near-Port sequence.

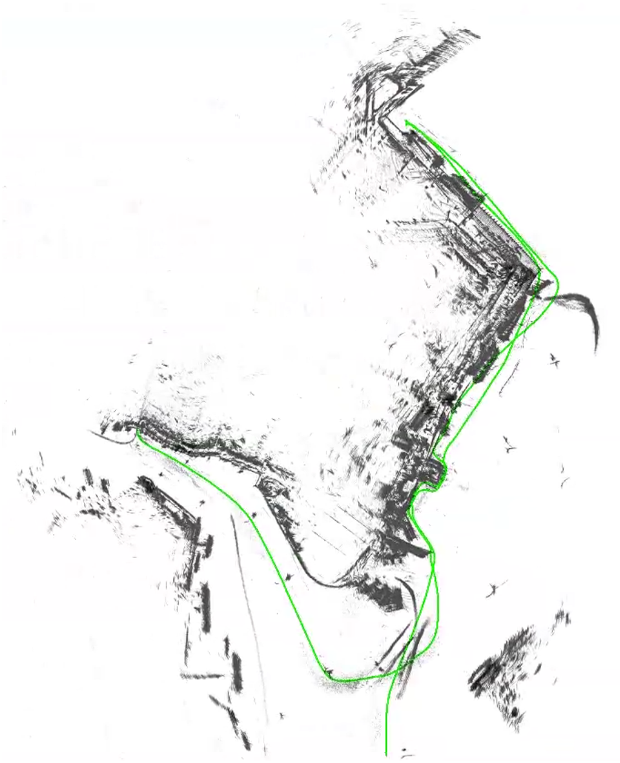

Figure 3 The mapping result of MRGF on Near-Port sequence.

Figure 2 illustrates the trajectory comparison between the proposed method and the ground truth on the Near-Port sequence. The estimated trajectory generally follows the overall shape of the reference path, indicating that the proposed framework is capable of maintaining stable localization in a large-scale maritime environment.

From the figure, it can be observed that the alignment between the two trajectories is relatively consistent along most segments, especially in the early and middle portions of the sequence. However, noticeable deviations appear in certain regions, particularly in areas with sharp turns or sparse structural features. These discrepancies suggest that while the proposed method achieves reliable local motion estimation, small errors may accumulate over time, leading to observable global drift. This phenomenon is common in radar-based SLAM systems operating in environments with limited geometric constraints and strong measurement noise.

Table 1 Relative trajectory error (RTE) on the Near-Port sequence of the MOANA dataset.

Method	RTE mean (m)	RTE RMSE (m)	RTE std (m)
Fusion (Ours)	0.66	1.67	1.53

Table 1 provides a quantitative evaluation of the proposed method in terms of relative trajectory error (RTE), which reflects the short-term motion consistency of the system. The results show that the proposed fusion framework achieves an RTE mean of 0.66 m and an RTE RMSE of 1.67 m, indicating that the system maintains relatively accurate local motion estimation over consecutive frames.

The moderate standard deviation (1.53 m) further suggests that the estimation remains stable without significant outliers, which can be attributed to the adaptive fusion strategy and the consistency-aware gating mechanism. These components effectively suppress unreliable measurements and prevent abrupt error propagation, especially under challenging maritime conditions.

Overall, the quantitative results are consistent with the qualitative observations in Fig. 2. While global deviations are still present due to long-term drift, the relatively low RTE demonstrates that the proposed method maintains strong local motion consistency. This behavior is particularly important for SLAM systems operating in large-scale and weakly constrained maritime environments.

4.4 Ablation and Analysis

Table 2 Relative trajectory error(RTE) on the nearport series of the MOANA dataset.

Method	RTE mean (m)	RTE RMSE (m)	RTE std (m)
CFEAR only	1.43	3.08	2.73
LodeStar only	0.99	0.85	1.30
Fusion	0.66	1.67	1.53

In Table 2, the results highlight the complementary characteristics of the two radar modalities. The CFEAR-only method exhibits relatively large errors (RTE RMSE = 3.08 m), indicating sensitivity to sparse structures and dynamic sea clutter. In contrast, the LodeStar-only method achieves lower RMSE (0.85 m), demonstrating strong rotational stability, but shows higher mean error and variance in certain segments, suggesting less consistent translation estimation due to the limited spatial resolution of X-band radar.

The proposed fusion method achieves a balanced performance, with an RTE RMSE of 1.67 m and a reduced mean error of 0.66 m. Although its RMSE is higher than that of LodeStar-only, the fusion approach provides more consistent and stable motion estimation by combining reliable translation from W-band radar with robust rotation from X-band radar.

These results indicate that the proposed method improves the stability and consistency of odometry, rather than optimizing a single metric, which is particularly important for long-term SLAM in challenging maritime environments.

In addition, the experimental results demonstrate that the proposed framework maintains stable performance under challenging maritime conditions, including sparse structural features, dynamic sea clutter, and long-range sensing scenarios. By leveraging complementary radar modalities, the system can effectively reduce estimation instability caused by environmental degradation, enabling more reliable odometry for long-term navigation tasks.

5 Acknowledge

This work was supported in part by the National Natural Science Foundation of China (Grant No. 42471480) and in part by the Key Research and Development Projects in Hubei Province (Grant No. 2024BAB078).

6 Conclusion

This paper presents a complementary multi-band radar SLAM framework for robust maritime localization. By fusing W-band and X-band radar, the method leverages their complementary characteristics to mitigate the limitations of single-band systems. A quality-aware adaptive weighting strategy and a consistency gating mechanism further enhance robustness under sensor degradation.

Experimental results on the MOANA dataset show that the proposed method achieves stable and reliable local motion estimation, with an RTE RMSE of 1.67 m on the Near-Port sequence, demonstrating its effectiveness in maintaining consistent odometry performance in challenging maritime environments.Future work will explore tighter integration with inertial sensing and improving robustness and accuracy across additional sequences of the MOANA dataset.

References

[1] C. Cadena, L. Carlone, H. Carrillo, Y. Latif, D. Scaramuzza, J. Neira, I. Reid, and J. J. Leonard, "Past, present, and future of simultaneous localization and mapping: Toward the robust-perception age," *IEEE Transactions on robotics*, vol. 32, no. 6, pp. 1309–1332, 2017.

[2] R. Mur-Artal, J. M. M. Montiel, and J. D. Tardos, "Orb-slam: A versatile and accurate monocular slam system," *IEEE transactions on robotics*, vol. 31, no. 5, pp. 1147–1163, 2015.

[3] J. Engel, T. Schöps, and D. Cremers, "Lsd-slam: Large-scale direct monocular slam," in *European conference on computer vision*. Springer, 2014, pp. 834–849.

[4] M. Bijelic, T. Gruber, F. Mannan, F. Kraus, W. Ritter, K. Dietmayer, and F. Heide, "Seeing through fog without seeing fog: Deep multimodal sensor fusion in unseen adverse weather," in *Proceedings of the IEEE/CVF conference on computer vision and pattern recognition*, 2020, pp. 11 682–11 692.

[5] D. Adolfsson, M. Magnusson, A. Alhashimi, A. J. Lilienthal, and H. Andreasson, "Lidar-level localization with radar? the cfear approach to accurate, fast, and robust large-scale radar odometry in diverse environments," *IEEE Transactions on robotics*, vol. 39, no. 2, pp. 1476–1495, 2022.

[6] D. Adolfsson, M. Magnusson, A. Alhashimi, A. Lilienthal, Achim J, and Henrik, "Cfear radarodometry-conservative filtering for efficient and accurate radar odometry," in *2021 IEEE/RSJ International Conference on Intelligent Robots and Systems (IROS)*. IEEE, 2021, pp. 5462–5469.

[7] H. Jang, M. Jung, M.-H. Jeon, and A. Kim, "Lodestar: Maritime radar descriptor for semi-direct radar odometry," *IEEE Robotics and Automation Letters*, vol. 9, no. 2, pp. 1684–1691, 2024.

[8] H. Zihang, L. Xiong, G. Zhuo, L. Gao, S. Lu, J. Zhu, and B. Leng, "4d radar-inertial slam based on factor graph optimization," SAE Technical Paper, Tech. Rep., 2024.

[9] V.-J. Štironja, J. Peršić, L. Petrović, I. Marković, and I. Petrović, "Movro2: Loosely coupled monocular visual radar odometry using factor graph optimization," *Robotics and autonomous systems*, vol. 184, p. 104860, 2025.

[10] H. Jang, W. Yang, H. Kim, D. Lee, Y. Kim, J. Park, M. Jeon, J. Koh, Y. Kang, M. Jung *et al.*, "Moana: Multi-radar dataset for maritime odometry and autonomous navigation application," *The International Journal of Robotics Research*, vol. 45, no. 2, pp. 193–203, 2026.

[11] S. H. Cen and P. Newman, "Precise ego-motion estimation with millimeter-wave radar under diverse and challenging conditions," in *2018 IEEE International Conference on Robotics and Automation (ICRA)*. IEEE, 2018, pp. 6045–6052.

[12] Z. Hong, Y. Petillot, and S. Wang, "Radarslam: Radar based large-scale slam in all weathers," in *2020 IEEE/RSJ International Conference on Intelligent Robots and Systems (IROS)*. IEEE, 2020, pp. 5164–5170.

[13] G. Kim and A. Kim, "Scan context: Egocentric spatial descriptor for place recognition within 3d point cloud map," in *2018 IEEE/RSJ International Conference on Intelligent Robots and Systems (IROS)*. IEEE, 2018, pp. 4802–4809.

[14] T. Qin, P. Li, and S. Shen, "Vins-mono: A robust and versatile monocular visual-inertial state estimator," *IEEE transactions on robotics*, vol. 34, no. 4, pp. 1004–1020, 2018.

[15] T. Shan, B. Englot, D. Meyers, W. Wang, C. Ratti, and D. Rus, "Lio-sam: Tightly-coupled lidar inertial odometry via smoothing and mapping," in *2020 IEEE/RSJ international conference on intelligent robots and systems (IROS)*. IEEE, 2020, pp. 5135–5142.